Resources and Environment 2022, 12(3): 88-97
DOI: 10.5923/j.re.20221203.03

Aerosols Characteristics in Two Cities Characterized by Different Levels of Air Pollution: Cairo and Qena/ Egypt

Khalafallah Omar Kassem[1,2,*], Eman Fouad El-Nobi[2]

[1]Physics Department, College of Science, Jouf University, Sakaka, Saudi Arabia
[2]Physics Department, Faculty of Science, South Valley University, Qena, Egypt

Abstract This paper introduces the aerosol characteristics in two cities, Cairo and Qena, Egypt. The two cities are characterized by different levels of air pollution. Aerosol characteristics are studied by comparing the aerosol optical depth (AOD) and angstrom exponent, α, as well as its second derivative, $\dot{\alpha}$. The used data are collected from the AERONET network constructed in the two cities. The results indicated that the two cities, Cairo and Qena, are characterized by different levels of air pollution and aerosol characteristics. Comparison of the AOD values at three wavelengths (340,500 and 870 nm) in Cairo and Qena, and comparison of the monthly mean distribution of Ångström wavelength exponent (α) at three wavelength bands (440–870, 440–675, and 675–870 nm), indicated the presence of a bimodal AOD distribution with primary and secondary maxima in April in both Cairo and Qena and in Nov in Cairo and in Oct in Qena. Results of the correlation between Angstrom wavelength exponent α computed at shorter (380-440 nm) and longer (675-870 nm) wavelengths in Cairo and Qena have shown that the curvature in Cairo is negative in 33% of total cases indicating the presence of fine mode aerosols, while in Qena, the curvature is rarely negative; 5% of total cases, indicating the presence of coarse-mode aerosols. Finally, values of the second derivative $\dot{\alpha}$ at Cairo and Qena are discussed as a function of AOD_{500} nm. In Cairo, Positive $\dot{\alpha}$ values indicate predominately fine mode bimodal size distributions with the value of $\dot{\alpha}$ increases as the fine mode increasingly dominates over the coarse and as the fine mode particles increase in size. While in Qena, the coarse mode dominated desert dust cases typically show $\dot{\alpha}$ values near zero or slightly negative.

Keywords Aerosol Optical Depth, Å ngström exponent, Qena, Cairo

1. Introduction

Numerous industrial and urbanization activities have been introduced in Egypt during the past few decades leading to increasing environmental problems, such as air pollution, particulate matter, gasses, and aerosols to high levels exceeding the world health organization (WHO) levels, especially in Cairo [1,2]. Atmospheric aerosols play an important role in climate, their radiative forcing, on a global average, is likely to be comparable in magnitude to the radiative forcing of about 2.4 W m−2 by anthropogenic greenhouse gases [3]. Nevertheless, their effect is difficult to estimate, mainly because there is incomplete knowledge of their optical properties [4,5], resulting thus in a large uncertainty regarding the aerosol overall radiative forcing [6-8]. This may be due to the difference in the degree of mixing and variability between the gasses and the aerosols in the atmosphere, gasses are well-mixed, while aerosols are inhomogeneous and have highly special and temporal variability. There are a rather limited number of general categories of aerosol types with distinct optical properties. In general, aerosols can be classified into the following four aerosol types, which are associated with different sources and emission processes, and they exhibit significantly different optical properties: 1) biomass-burning aerosols, produced by forest and grassland fires, 2) urban/industrial aerosols from fossil fuel combustion in populated urban/industrial regions, 3) desert dust blown into the atmosphere by wind, and 4) aerosols of maritime origin. [9]

Aerosol optical depth AOD (τ_λ) represents the extinction of radiation at wavelength λ resulting from the atmospheric aerosols [10]. The wavelength dependence of AOD varies between different aerosol types because of their different physical and chemical characteristics. AOD wavelength dependence is expressed by the Angstrom exponent α which is the slope of the wavelength dependence of the AOD in logarithmic coordinates [11].

$$\alpha_{(\lambda_1,\lambda_2)} = -\ln(\frac{\tau_{\lambda 2}}{\tau_{\lambda 1}})/\ln(\frac{\lambda_2}{\lambda_1}) \quad (1)$$

Within the solar spectrum α can be used as an indicator for the size of the atmospheric aerosols determining the AOD: α>0 is mainly determined by fine mode, submicron aerosols.

* Corresponding author:
kokassem@ju.edu.sa (Khalafallah Omar Kassem)
Received: Nov. 8, 2022; Accepted: Nov. 15, 2022; Published: Dec. 6, 2022
Published online at http://journal.sapub.org/re

While α<1 is largely determined by coarse or supermicron particles. It is well known that large fine mode particles can have the same α as mixtures of coarse mode and small fine mode ones so that α alone does not provide unambiguous information on the relative weight of coarse and fine modes in determining the AOD [10].

For several years great effort has been devoted to the study of the spectral variation of the Angstrom exponent α for extracting information about the aerosol size distribution [10,12-19]. For example, the negative values of the difference α(440, 613)-α(4440, 1003) refer to the dominance of fine mode aerosols, while the positive difference refers to the effect of two separate particles modes. Also, in the wavelength range 380-870 nm, α can increase by a factor of 2-5 as wavelength increases for biomass burning and urban aerosols, while remaining constant or decreasing in the presence of mineral dust [15]. In 2006, [19] addressed the link between Angstrom exponent curvature (second derivative of α) and the ratio between fine and total aerosol volume.

Most Aerosol studies in Egypt are concentrated on Cairo and the Nile delta, for instance [20-29]. Marey, H.S. et al 2011 in [20] studied the optical and microphysical aerosol properties over the Nile Delta using satellite data. They found significant monthly variability in the AOD with maxima in April or May (~0.5) and October (~0.45), and a minimum in December and January (~0.2). They found spherical aerosols during the black cloud periods characterized by a higher percentage of small and medium-size particles, whereas the aerosols during spring are generally large non-spherical particles. Also, they concluded that the region of Cairo and the Nile is subject to a complex mixture of air pollution types, especially in the fall season, when biomass burning contributes to a background of urban pollution and desert dust. [21] studied the reasons for the severe air pollution phenomenon occurrence known as the 'black cloud," in Cairo in the early autumn. They concluded that the cause of those events is the burning of agricultural waste after harvest season in the Nile delta region. El-Askary 2006 in [22] found that aerosol optical depth (AOD) behavior showed a dual maxima nature in each year from 2000 till 2005 during the months of (April, May) and October attributed to dust and air pollution events, respectively. Such behavior is confirmed by the high negative correlation with the aerosol fine mode fraction reaching -0.75. Aerosol fine mode fraction product confirmed by a high value in October represented the Black Cloud episodes due to fine particles contribution in these events rather than during the dust events. They confirmed burns' contribution to the Black Cloud formation. El-Askary et al 2008 in [23] have also studied dust storms, dense haze, and the black cloud that occurred over Cairo and the Nile delta during the spring and autumn months for the period from 2004 to 2006. They concluded that the observed pollution accumulation is a result of temperature inversion conditions, as well as adverse weather conditions. In addition, Prasad, A.K. et al 2010 in [24] found that the black cloud is affected also by long-range transport of dust at high altitudes (2.5-6 km) from Western Sahara and its deposition over the Nile Delta region. Also, El-Askary et al 2009 in [25] stated that the weather conditions prevailing in the Mediterranean Sea result in a westerly wind flow pattern during spring and from North to South during the summer. They confirmed that such flow patterns transport dust-loaded and polluted air masses from the Sahara desert and Europe, respectively, through Alexandria and the Nile Delta in Egypt. Measurements declared a seasonal variability in aerosol optical depth (AOD) following these flow patterns. The results obtained by El-Metwally, M. et al 2008 in [26] suggest that the variations in the overall aerosol properties are due to changes in the proportions of the mixture consisted of. In particular, short-duration dust storms and biomass-burning episodes explain the largest observed aerosol optical depths (AOD) (AOD > 0.7) through the extreme enhancements of concentrations in dust-like aerosols characterized by low Ångström's exponent values (alpha < 0.5) and in "biomass-burning" aerosols (1.0 < alpha < 1.5). Also, Elmetwally et.al (2011) in [27], using the analysis of the temporal variation of the AOD and spectral dependence, suggested that the aerosols in Cairo are generally a mixture of at least three main components differing in composition and size: 1) a highly absorbing background aerosol produced by daily activities such as traffic and industry, 2) an additional, 'pollution' component produced by the burning of agricultural wastes in the Nile delta, and 3) a coarse desert dust component. Recently, Islam Abou El-Magd et al. (2020) in [28] investigated the AOD and for the period 2012–2018 in Cairo. They concluded that the summer and autumn seasons experienced the highest anomaly originating from regional and national sources. They also found that the high AOD and low Ångström exponent (AE) in spring indicated the presence of coarse particles which naturally originate from desert dust or sea spray. In contrast, the high AE in summer and autumn resulted from the dominance of fine anthropogenic aerosols such as smoke particles from local biomass burning. Also, Wenzhao Li et al. 2019 in [29] found that most of the severe aerosol events are caused by dust or mixed related scenarios in Cairo and the Nile delta during the spring, fall, and summer. Whereas during winter aerosols of finer size lead to severe heavy conditions.

In Qena, a few number of studies have been concerned with the Total Particulate Matter (TPM) and AOD characteristics such as [30-32]. In [30,31] they studied the temporal variation of particulate matter (PM_{10}) concentrations and its affect by the meteorological parameters. Results indicated that the average mass concentration of total suspended particulate matter was 158.3 ± 40.1 μg/m^3, the winter average value was 182.5 μg/m^3, while the summer average value was 132.5 μg/m^3. In the entire study period, TPM particles have irregular, spherical and aggregated shapes. Also, they analyzed the chemical constituents of the TPM. Elemental analysis indicates that C, Si, and Ca were the abundant elements in the particles

followed by Al, Na, and Fe. In addition, the study utilized the AOD level measured from satellite data. In [32] the effect of long-range transport on the particulate matter concentration in Qena is studied. The study revealed that most air mass trajectories are found in the northern clusters during the whole period as well as during spring, summer, and autumn. North Africa and the southwest of Turkey are found to be the most probable sources of PM_{10} during spring and all the study period.

2. Study Area, Data, and Methodology

Egypt, as shown in figure (1), is located northeast of Africa and consists mainly of two desert plateaus separated by the narrow Nile valley. The western desert is larger than the eastern desert. The Nile valley becomes large in the north and forms the Delta; the main agricultural area in Egypt. Cairo is located at the beginning of the branching of the Nile into the Rashid and Damietta branches. Due to the huge desert areas and the large population as well as increased industrialization, the common sources of the aerosols in Egypt can be classified as (1) sand and dust particles blown from desert areas, especially during the windy season (spring) [33], (2) Sea salt from the Mediterranean Sea transported by northern and north-west air masses (31Kassem, Kh. O. 2008), (3) biomass burning in the Nile valley and the delta, (4) local activities from industrial and urbanized areas. Cairo is the capital of Egypt and the largest and most important city in Egypt. It is the largest Arab city in terms of population and area, and occupies the second place in Africa and seventeenth in the world in terms of population, with a population of 21,322,750 million people according to statistics in 2021. They represent 20% of the total population of Egypt. Qena is located in Upper Egypt 600 km south of Cairo, east of the Nile River. It is the capital of Qena Governorate and its largest city, its population is 350 thousand people.

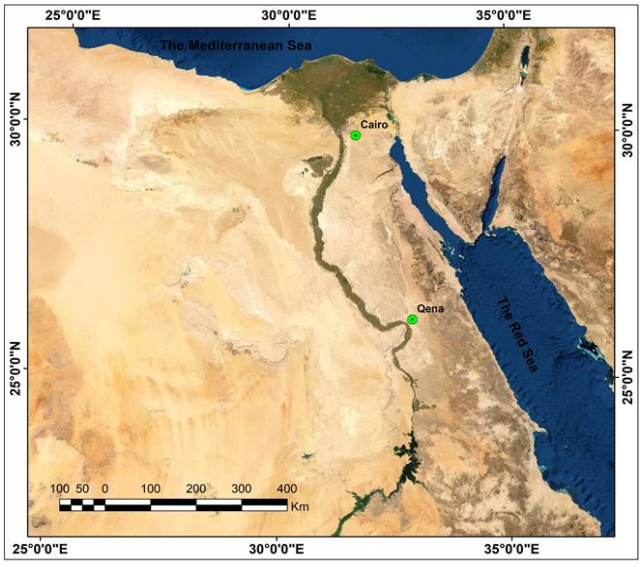

Figure 1. Map of Egypt

AERONET is a ground-based aerosol network set up by the National Aeronautics and Space Administration (NASA) and LOA-PHOTONS Centre National de la Researche Scientifique (CNRS) and is significantly extended by associates from national offices, foundations, colleges, singular researchers, and accomplices. AEROENT data is characterized by its high frequency (every 15 min) and low uncertainty observations [29]. Instantaneous AOD values of quality-assured level 2.0 data were acquired from the AERONET station of "Cairo_EMA_2" located at 30.081° N, 31.290° E. and "Qena_SVU located at 26.20 N, 32.75 E". AERONET data are available at https://aeronet.gsfc.nasa.gov. The data are automatically cloud cleared and quality assured with pre-field and post-field calibration applied. AOD is measured at seven wavelengths 340nm, 380nm, 440nm, 500nm, 675nm, 870nm, and 1020nm.

Angstrom exponent (AE) can be calculated using the spectral variation of AOD by applying the Volz method (Equation (1)) to distinguish the different aerosol types [35,36]. For comparison between the two locations, Cairo and Qena, we used the available instantaneous 11 months data in Qena during the period from 12/22/2018 to 10/22/2019 and the corresponding year-round period of data in Cairo during the period from 8/2/2018 to 7/30/2019.

In this work, we compared the monthly mean values of AOD at three wavelengths (340,500 and 870 nm) in Cairo and Qena. Also, the monthly mean distribution of Å ngström wavelength exponent (α) at three wavelength bands (440–870, 440–675, and 675–870 nm) is calculated and compared in the two cities. In addition, the values of Angstrom wavelength exponent α computed at shorter (380-440 nm) and longer (675-870 nm) wavelengths in Cairo and Qena are calculated for clarifying positive (concave type) and negative (convex type) curvature in the two cities. The correlation between the differences of Angstrom exponent and AOD at 500 nm is studied in the two cities. Finally, values of the second derivative computed from instantaneous values of 380, 500, and 870 nm at Cairo and Qena as a function of nm are discussed.

3. Results and Discussion

Figure (2) shows the monthly mean variation of AOD values at three wavelengths (340,500 and 870 nm) in Cairo and Qena using Box and Whisker plots. In Cairo, the values increased from low values (0.21 -0.38) in Jan to record relatively high values (0.33—0.55) and (0.26 – 0.74) in April and Nov., respectively. While in Qena, the values increase gradually from (0.07-0.13) in Dec. to a maximum value (0.27 – 0.31) in April, then decrease from April to (0.12 – 0.20) in Aug, after that increases again to (0.17 – 0.28) in Oct. These behaviors illustrate a bimodal AOD distribution with primary and secondary maxima in April in both Cairo and Qena and in Nov in Cairo and in Oct in Qena (There is no available data in Nov. in Qena). The results thus obtained are compatible with the maximum values of AOD found by [27]

in April and Oct. and with the results found by [28] in Cairo. The large range of Box for AOD340 in Feb and Nov in Cairo gives a sign of large variability in the fine mode aerosols, while the large range of Box for AOD870 in April and Nov gives a sign of large variability in the coarse mode aerosols. This result also is following that found by [28], who found that in May and Oct, there was a pronounced presence of AOD, using daily data of MODIS over Egypt. They stated that the source of the coarse mode aerosols is the dust storms that frequently occur in spring due to the prevalent Khamasin wind in this season. In Qena, there is a pronounced range of the Box for AOD340 and AOD870 in April and May, indicating a large variability in the fine and coarse mode aerosols. The monthly mean values of AOD340 are greater than that of AOD500 and AOD870 in all the months in Cairo and Qena. The significant monthly variation in the range of AOD at particular wavelengths indicates more or less homogeneity in the aerosol burden. The large intra-monthly variability in aerosol burden exhibits in April and May in Qena and in Nov in Cairo. In Qena this is the time of Khamasin winds and sugar cane agricultural wastes burning, while in Cairo, it is the time of black cloud formation due to the rice agricultural wastes burning [28]. The large range of Box for AOD340, AOD 500, and AOD 870 in Qena during April and May gives a sign of large variability in the fine and coarse mode aerosols during those two months, while this case is more pronounced in Nov in Cairo, although all the months in Cairo are characterized by pronounced ranges of Box in comparison with that in Qena. In addition, throughout the year, there is a large range of AOD340 boxes compared to AOD500 and AOD870 in Cairo, indicating the presence of fine mode aerosol burden in the atmospheric column and expressing the influence of anthropogenic aerosol. this case is found to a less extent in Qena.

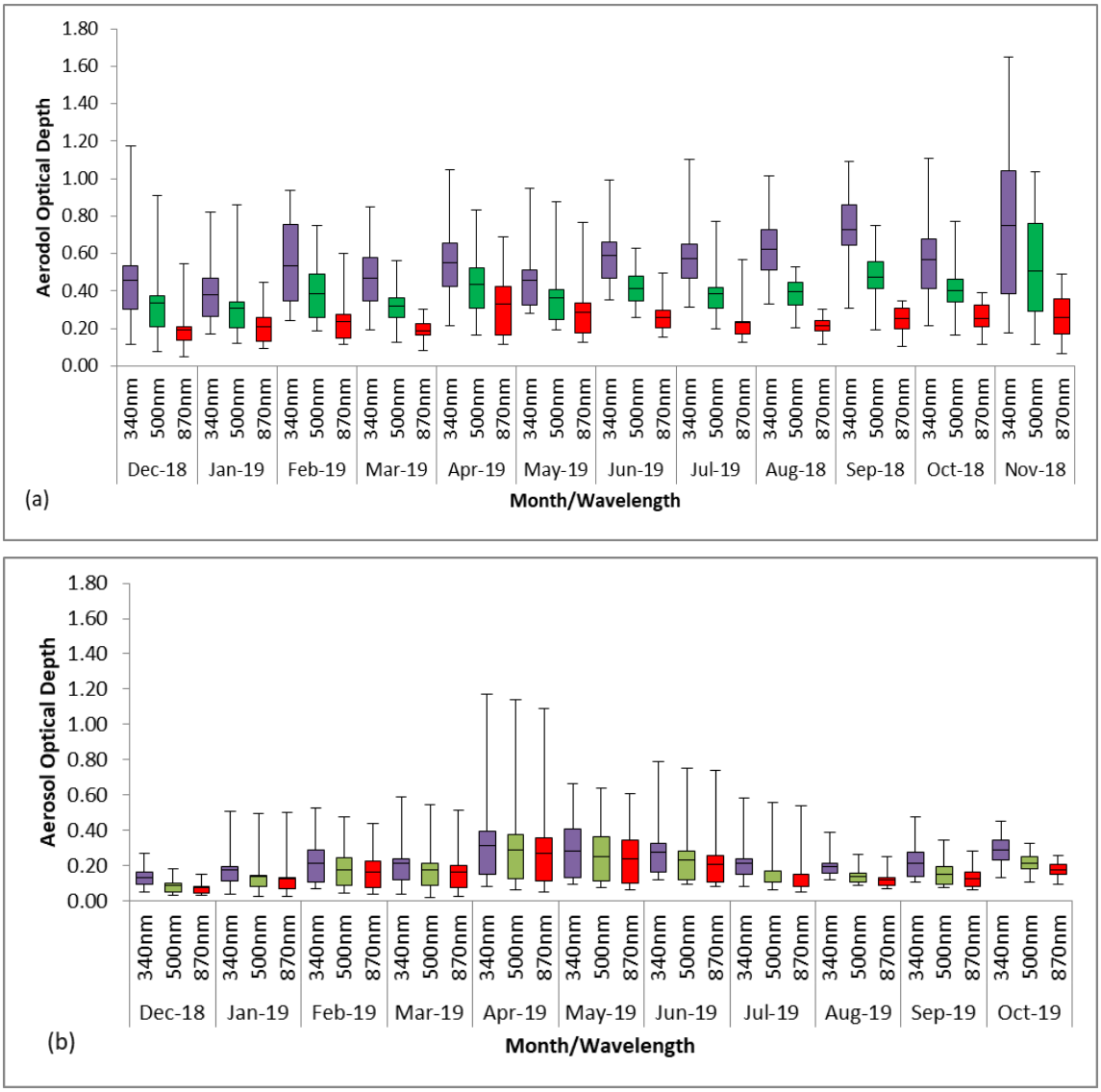

Figure 2. Monthly mean distribution of spectral aerosol optical depth at 340 nm, 500 nm, and 870 nm in Cairo (a) and Qena (b). Upper and lower whiskers represent the maximum and minimum values, respectively, Upper and lower ends of the box represent the third and first quartiles, respectively, and the interior horizontal line represents the mean values

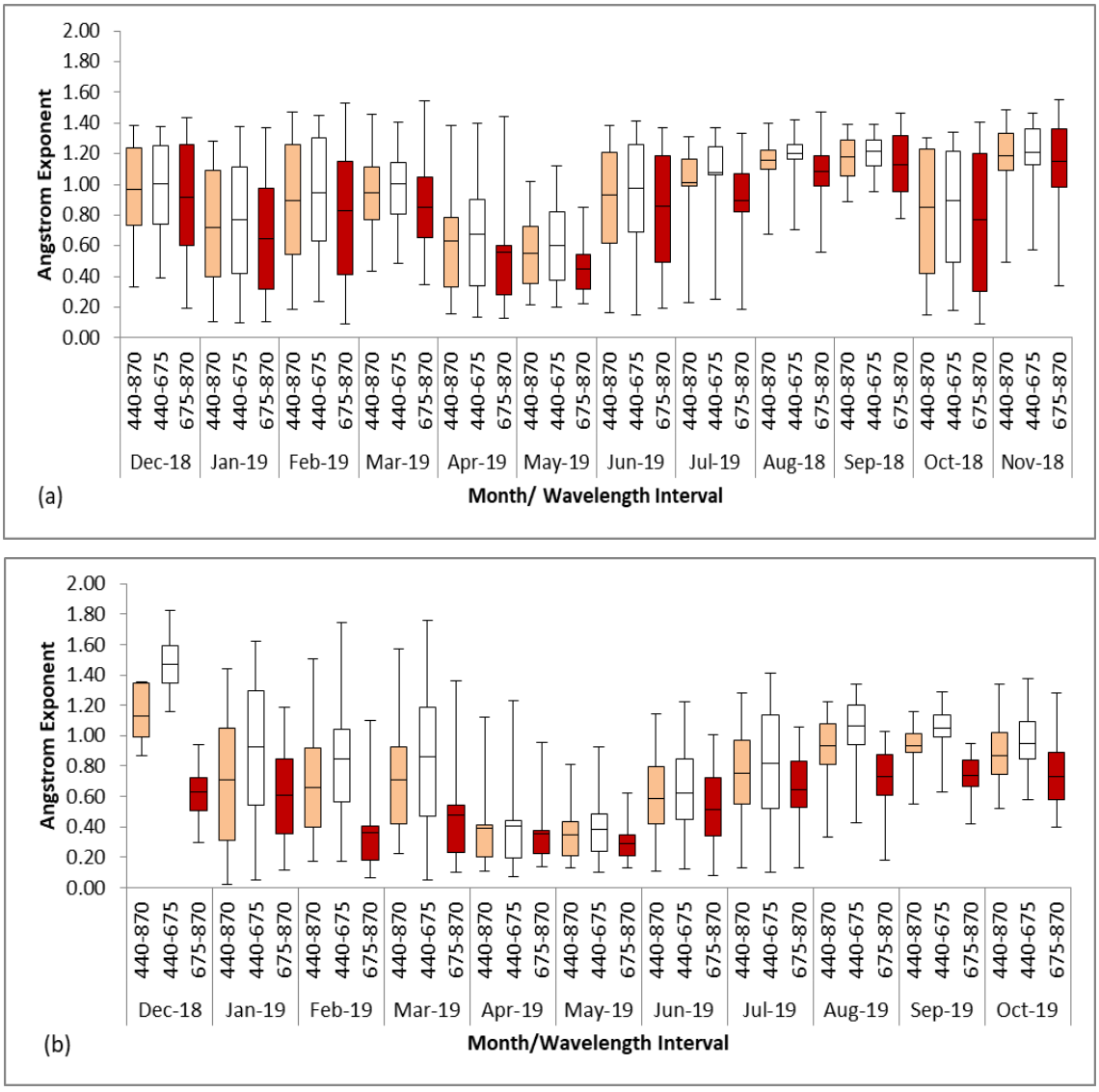

Figure 3. Monthly mean distribution of Ångström wavelength exponent (α) at three wavelength bands (440–870, 440–675, and 675–870 nm) in Cairo (a) and Qena (b). Upper and lower whiskers represent the maximum and minimum values, respectively, Upper and lower ends of the box represent the third and first quartiles, respectively, and the interior horizontal line represents the average values

Figure (3) illustrates the monthly mean distribution of α values at three wavelength bands (440–870 nm, 440–675 nm, and 675–870 nm) in Cairo and Qena. The difference in α values between short and long-wavelengths defines the sign and magnitude of the curvature [19], while the inter-band variation of α values in short and long wavelengths provides information about the variation in fine-mode radii and fine-mode fraction, respectively. In the two cities, there is a clear decrease in α value from winter (Dec) to spring (May), then, an increase again from summer to autumn. The minimum values of α occurred in April-May in the two cities indicating clear dominance of coarse-mode aerosols transported from the desert along with marine aerosols transported with long-range air mass from the Mediterranean Sea and Atlantic ocean as stated in [34]. In Cairo, the values generally decrease from relatively high values (1.15 – 1.21) and (0.91 – 1.0) in Nov and Dec, respectively, to low values (0.45 – 0.61) in May, then increase from May to Nov. The high values of the Angstrom exponent in autumn indicate the presence of fine mode aerosols resulting from fires in the rice crop wastes in the delta [28]. There is an abrupt decrease in α values in the two months Jan (0.64-0.77) and Oct (0.77 – 0.85). In Qena, the values decrease from maximum values occurred in Dec (0.62-1.12) to minimum value (0.29-0.38) in May, then, increase to relatively high values (0.73-1.06) in Aug, after that, decreases to (0.73 – 0.95) in Oct. During the whole period of the study in the two cities, we can notice a large value of $\alpha_{440-675}$ compared to $\alpha_{675-870}$ with the difference between the two values is larger in Qena compared to that in Cairo. This Indicates clear positive curvature and clear dominance of coarse particles in Qena. The phenomenon is less pronounced in Cairo due to a large amount of local anthropogenic particles. In Both Cairo and Qena, we can notice that mean values of α at long wavelength interval (675-870) nm are less than the mean α at short wavelength interval (440-675) nm in the whole period of study. This is due to the presence of mineral dust in the two cities, especially in Qena, where the differences are

more significant [15].

Based on the spectral dependence of α and its relationship with atmospheric turbidity stated by many authors such as [37], the values of α in Cairo and Qena were computed in two narrow spectral intervals, 380-440 and 675-870 nm by applying the Volz method. The correlation between α values computed in the two mentioned narrow spectral bands is shown in figure (4) for the two cities, Cairo and Qena. In this figure we can notice the followings; first, the relationship between α-values in the two spectral intervals is not linear in the two cities as few points are laying on the one-to-one line. This result is following that reported by (34Kaskaoutis D. G. et al, 2007) in four AERONET stations representing different kinds of aerosols. In this case, points located in the upper part of the plot represent negative curvature $\alpha_2 < 0$ and indicate the presence of fine mode aerosols, while, points located in the lower part of the figure $\alpha_2 > 0$ represent positive curvature and indicate the presence of coarse-mode aerosols. So, it is found that the curvature in Cairo is negative ($\alpha_2 < 0$) in 33% of total cases, while in Qena, the curvature is rarely negative; 5% of total cases. This result reflects the difference between the nature of the aerosol load in a big –urban city such as Cairo and a relatively small city characterized by a relatively clean atmosphere in comparison with that of Cairo. In addition, the difference in the AERONET stations located in the two cities; in Cairo, it is located in the middle of the city, while in Qena, it is located in a suburb desert region far away from the pollution sources. From the figure we can see that both Cairo and Qena are affected by the coarse mode aerosols generated from the desert surrounding them; Cairo is affected in 67% of the total cases while Qena is affected in 95% of the total cases. These results are following that found in Altafloresta (Urban city) and Solar village (dessert), respectively, [37].

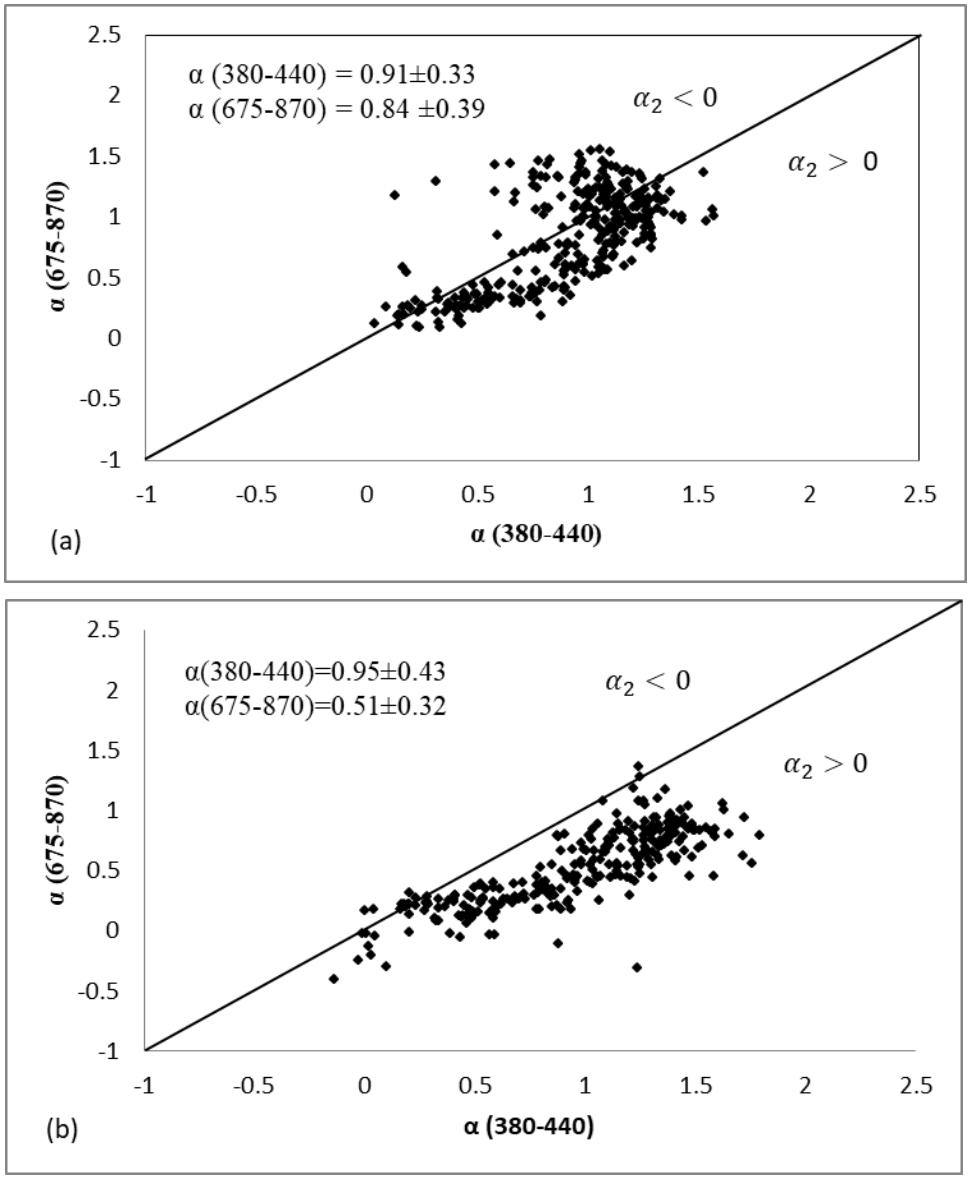

Figure 4. Regression between the values of Angstrom wavelength exponent α computed at shorter (380-440 nm) and longer (675-870 nm) wavelengths for the two sites (a) Cairo and (b) Qena. The one-to-one line is also shown together with α_2 values implying positive (concave type) and negative (convex type) curve related to equation 5

Equations (2) and (3) illustrate the correlation coefficients between the α values of Angstrom exponent computed at a shorter wavelength (380-440 nm) and longer wavelength (675-870 nm) in Cairo and Qena.

$$\alpha_{(675-870)} = 0.80\,\alpha_{(380-440)} + 0.11 \quad R2=0.44 \text{ (Cairo)} \quad (2)$$

$$\alpha_{(675-870)} = 0.59\,\alpha_{(340-440)} - 0.0602 \quad R2=0.66 \text{ (Qena)} \quad (3)$$

The mean values and the standard deviation of α computed at a shorter wavelength (380-440 nm) and longer wavelength (675-870 nm) are illustrated also in figure 4, it is found that the mean value of α at a longer wavelength is slightly smaller than that at a shorter wavelength in Cairo, while it is significantly smaller in Qena. This result indicates that the curvature depends on the difference of α values computed in short and long wavelengths.

For illustrating the spectral variability of atmospheric exponent α and its dependence on atmospheric turbidity and aerosol type, the relationship between the difference of α values $\alpha_{380-440}$ and $\alpha_{675-870}$ as a function of atmospheric turbidity represented as means of AOD_{500} is shown in figure (5) for the two cities. In this figure, positive and negative differences are indicative of positive and negative curvatures, respectively. While differences near zero indicate the absence of the spectral variability in the Angstrom exponent. In this figure, we can notice that in Cairo, there is an increase in the range of differences with increasing turbidity. The differences become negative as the atmospheric turbidity increases as a result of increasing the fine mode particles ratio. This result is following that found in Alta Floresta [37]. We can notice that in Cairo, the differences are purely negative for small turbidity: AOD ranges from 0.1 to 0.2. Negative differences increase for AOD range from 0.2 to 0.7. Then, most of the differences become negative for AOD greater than 0.7. In Qena, the differences are positive for most cases, as shown in figure 4 (b), while the differences tend to be zero for high turbid dust conditions, with AOD larger than 0.5. This result is following that found by [15,37].

To characterize the departure from linearity of the ln τ_a versus ln λ relationship (Angstrom exponent) in the two cities, we utilize the parameter $\dot{\alpha}$ (the second derivative of α) defined by [15] as the derivative of α concerning ln λ. The parameter $\dot{\alpha}$ is computed from the relation:

$$\dot{\alpha}(\lambda_i) = \frac{d\alpha}{d\,ln\lambda} = -\left[\frac{2}{\ln \lambda_{i+1} - ln\lambda_{i-1}}\right]\left[\frac{ln\tau_{ai+1} - ln\tau_{ai}}{ln\lambda_{i+1} - ln\lambda_i} - \frac{ln\tau_{ai} - ln\tau_{ai-1}}{ln\lambda_i - ln\lambda_{i-1}}\right] \quad (4)$$

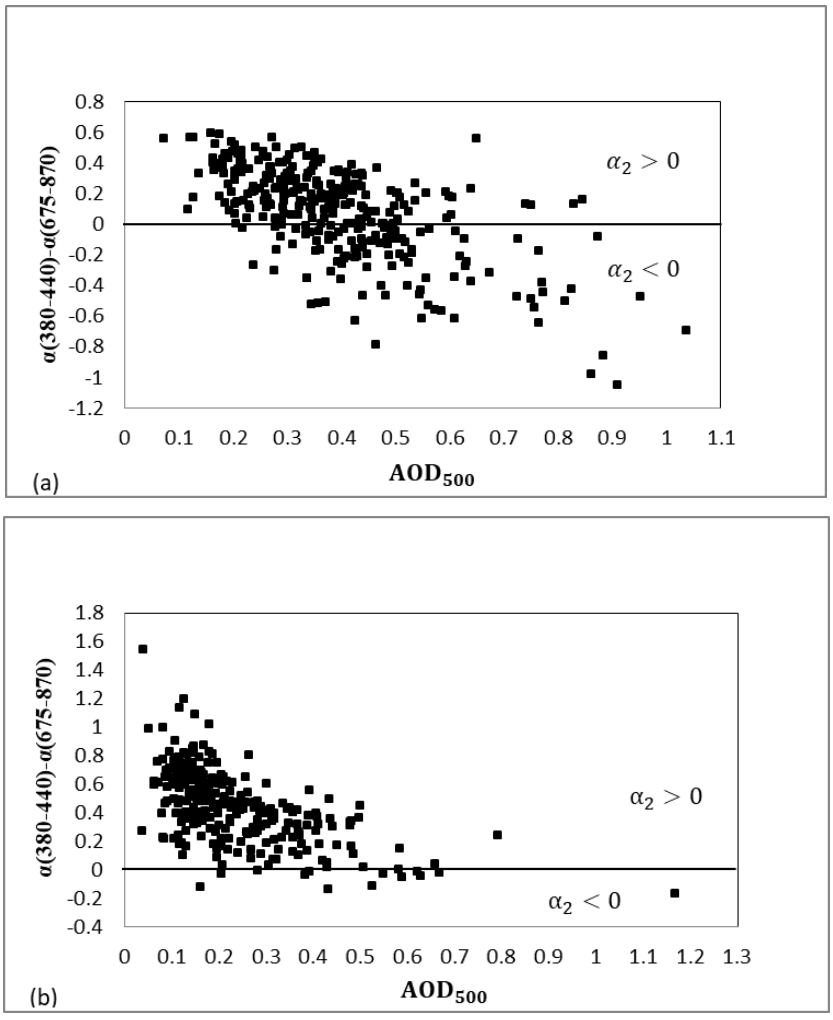

Figure 5. Correlation between the differences of Angstrom exponent, $\alpha_{380-440}$ - $\alpha_{675-870}$ and AOD for the two sites (a) Cairo and (b) Qena

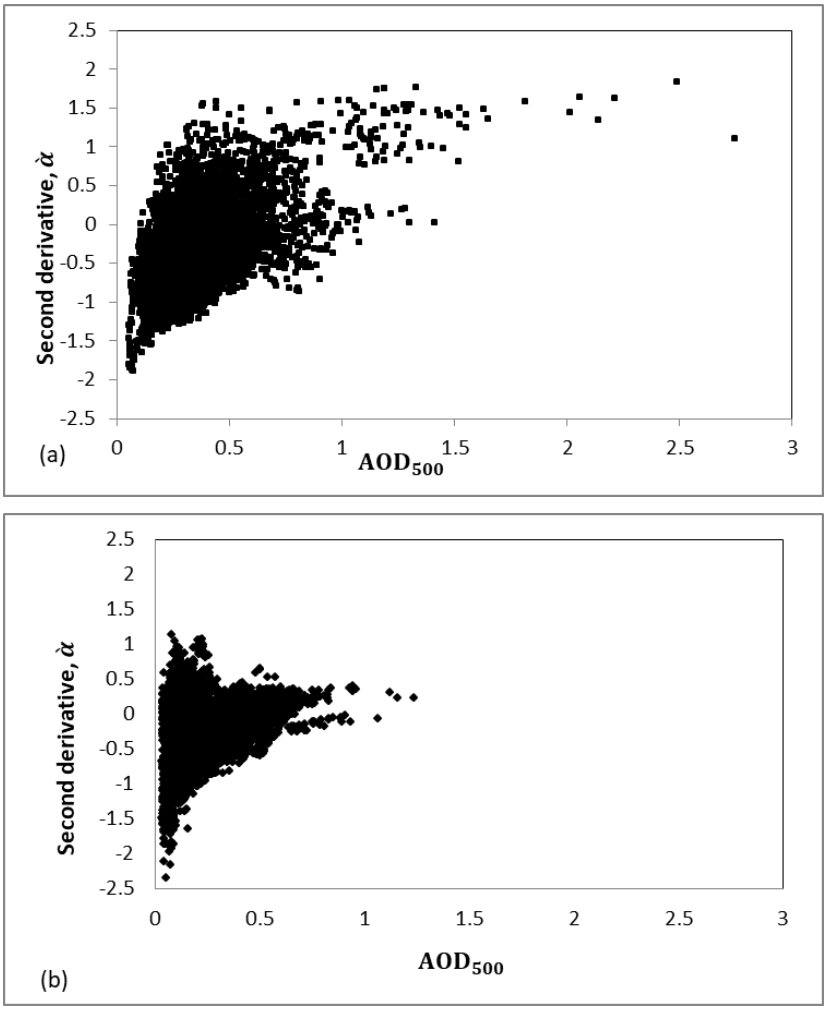

Figure 6. Values of the second derivative $\dot{\alpha}$ computed from instantaneous values of τ_a at 380, 500, and 870 nm at Cairo (a) and Qena (b) as a function of AOD_{500} nm

The parameter $\dot{\alpha}$ is a measure of the rate of change of the Angstrom exponent with the logarithm of the wavelength. Figure (6) represents the relationship between the instantaneous values of $\dot{\alpha}$ and the AOD 500 during the same period of the study. When $\dot{\alpha}$ is equal to zero there is no curvature in the ln τ_a versus ln λ relationship and therefore the Angstrom expression fits the data best.

As shown in Cairo, Figure. (6, a), which is characterized by fine mode urban aerosols, there is a tendency toward large positive values of $\dot{\alpha}$, especially as AOD500 increases, due to the strong optical influence of fine-mode particles at the higher optical depth [37]. Positive $\dot{\alpha}$ values typically occur in predominately fine mode bimodal size distributions with the value of $\dot{\alpha}$ increasing as the fine mode increasingly dominates over the coarse mode and as the fine mode particles increase in size [15,38-40]. In Qena we can see that the values of the differences are more close to zero, as shown in Figure (6, b), indicating the presence of coarse particles, since this site is strongly influenced by desert dust. It is found that the coarse mode dominated desert dust cases show $\dot{\alpha}$ values near zero or slightly negative [15,16]. Negative $\dot{\alpha}$ occurs when α (380 - 500 nm) is larger than α (500-870). This occurs as a result of bimodal size distributions at relatively low optical depths, with fine mode particles dominating the wavelength dependence of AOD at short wavelengths and coarse mode particles dominating the wavelength dependence at longer wavelengths [16]. From figure (6 a,b) we can conclude that both Cairo and Qena are affected by the desert dust coarse particles that make $\dot{\alpha}$ negative.

4. Conclusions

Summing up the results, it can be concluded that from the comparison of the monthly mean values of AOD at three wavelengths (340,500 and 870 nm) in Cairo and Qena, and the monthly mean distribution of Å ngström wavelength exponent (α) at three wavelength bands (440–870, 440–675 and 675–870 nm), there is a bimodal AOD distribution with primary and secondary maxima in April in both Cairo and Qena and in Nov in Cairo and Oct in Qena. In addition, the correlation between Angstrom wavelength exponent α computed at shorter (380-440 nm) and longer (675-870 nm) wavelengths in Cairo and Qena indicated that the curvature in Cairo is negative in 33% of total cases indicating the

presence of fine mode aerosols, while in Qena, the curvature is negative only in 5% of total cases, indicating the presence of coarse-mode aerosols. The correlation between the differences of Angstrom exponent, $\alpha_{380-440}$ - $\alpha_{675-870}$ and AOD at 500 nm is studied in the two cities. In Cairo, there is an increase in the range of differences with increasing the turbidity and the differences become negative as atmospheric turbidity increases as a result of increasing fine mode particles ratio. In Qena, the differences are positive for almost all cases, indicating the presence of coarse mode particles. Finally, values of the second derivative $\dot{\alpha}$ at Cairo and Qena as a function of AOD_{500} nm are discussed. In Cairo, Positive $\dot{\alpha}$ values occur in predominately fine mode bimodal size distributions with the value of $\dot{\alpha}$ increasing as the fine mode increasingly dominates over the coarse and as the fine mode particles increase in size. While in Qena, coarse mode dominated desert dust cases typically show $\dot{\alpha}$ values near zero or slightly negative. Although Cairo and Qena differ in Aerosol properties due to the difference in air pollution levels and sources in each city, the two cities are affected by the desert aerosols during spring months and biomass burning during autumn months.

ACKNOWLEDGEMENTS

The authors would like to thank and acknowledge the two PIs, Emilio Cuevas-Agullo, and Ashraf Zakey, for their effort in establishing and maintaining the Cairo_EMA_2 AERONET site, and the two PIs Ashraf_Zakey, _and_Mohamed_Hussein_Korany for their effort in establishing and maintaining the Qena_SVU AERONET site.

REFERENCES

[1] Aboel Fetouh, Y., El Askary, H., El Raey, M., Allali, M., Sprigg, W.A., Kafatos, M., Annual Patterns of Atmospheric Pollutions and Episodes over Cairo Egypt, Adv. Meteorol., 2013, 1-11, 984853. J. Thilagan, S. Gopalakrishnan, T. Kannadasan, A study on adsorption of Copper (II) ions in aqueous solution by Chitosan reinforced by Banana stem fibre, International Journal of Green and Herbal Chemistry, 2013, 2(2), 226-240.

[2] Moussa, M. and Abdelkhalek, A., Meteorological Analysis for Black Cloud (Episodes) Formation and Its Monitoring by Remote Sensing, J. Appl. Sci. Res., 2007, 3, 147–154. Gupta Vikal, Kulshreshtha Ruchi and Magan Lal, Effects of sodium dodecyl sulphate on biooxidation of copper mine tailings by acidithiobacillus ferroixidans, Res. J. Chem. Environ, 2010, 14(3), 51.

[3] Intergovernmental Panel on Climate Change (IPCC) (2001), Climate Change 2001: The Scientific Basis, edited by J. T. Houghton et al., 896 pp., Cambridge Univ. Press, New York.

[4] Houghton, J. T., Miera Filho, L. G., Callander, B. A., Harris, N., Kattenberg, A., and Maskell, K., Climate Change 1995: The Science of Climate Change: Intergovernmental Panel on Climate Change, Cambridge Univ. Press, p 552, 1996.

[5] Hansen, J., Sato, M., Ruedy, R., Lacis, A., and Oinas, V., Global warming in the twenty-first century: An alternative scenario, Proc. Natl. Acad. Sci., USA, 2000, 97, 9875–9880.

[6] Granger Morgan, M., Adams, P. J., and Keith, D. W., Elicitation of expert judgments of aerosol forcing, Clim. Change, 2006, 75, 195–214.

[7] Remer, L. A. and Kaufman, Y. J., Aerosol direct radiative effect at the top of the atmosphere over cloud free ocean derived from four years of MODIS data, Atmos. Chem. Phys., 2006, 6, 237– 253.

[8] Yu, H., Kaufman, Y. J., Chin, M., Feingold, G., Remer, L. A., Anderson, T. L., Balkanski, Y., Bellouin, N., Boucher, O., Christopher, S., DeCola, P., Kahn, R., Koch, D., Loeb, N., Reddy, M. S., Schulz, M., Takemura, T. and Zhou, M., A review of measurement-based assessment of aerosol direct radiative effect and forcing, Atmos. Chem. Phys., 2006, 6, 613–666, http://www.atmos-chem-phys.net/6/613/2006/.

[9] Twomey, S. Atmospheric Aerosols, Elsevier Scientific Publishing, Co.: New York, NY, USA, 1977.

[10] Gobbi G. P., Y. J. Kaufman. Koren, and T. F. Eck, 2007, Classification of aerosol properties derived from AERONET direct sun data. Atmos. Chem. Phys., 2007, 7, 453–458.

[11] Angstrom, A. K., On the atmospheric transmission of sun radiation and on the dust in the air, ¨Geogr. ANN., 1929, 12, 130–159.

[12] King, M. D., Byrne, D. M., Herman, B. M., Aerosol size distribution obtained by inversion of spectral optical depth measurements, J. Atmos. Sci.,1978, 35, 2153–2167.

[13] Nakajima, T., Takamura, T., Yamano, M., Consistency of aerosol size distributions inferred from measurements of solar radiation and aerosols, J. Met. Soc. Jap., 1986, 64, 765–776.

[14] Kaufman, Y. J., Aerosol optical thickness and atmospheric path radiance, J. Geophys. Res., 1993, 98(D2), 2677–2692.

[15] Eck, T. F., B. N. Holben, J. S. Reid, O. Dubovik, A. Smirnov, N. T. O'Neill, I. Slutsker, and S. Kinne, Wavelength dependence of the optical depth of biomass burning, urban, and desert dust aerosols, J. Geophys. Res., 1999, 104, 31, 333 – 31,349.

[16] O'Neill, N. T., Dubovik, O., and Eck, T. F., A modified Angstrom coefficient for the characterization of sub-micron aerosols, Appl. Opt., 2001a, 40, 2368–2375.

[17] O'Neill, N. T., Eck, T. F., Holben, B. N., Smirnov, A., and Dubovick, O., Bimodal size distribution influences on the variation of Angstrom derivatives in spectral and optical depth space, J. Geophys. Res., 2001b, 106(D9), 9787–9806.

[18] O'Neill, N. T., Eck, T. F., Smirnov, A., Holben, B. N., and Thulasiraman, S., Spectral discrimination of coarse and fine mode optical depth, J. Geophys. Res., 2003, 108(D17), 4559, doi:10.1029/2002JD002975.

[19] Schuster, G.L., Dubovik, O., Holben, B.N., Angstrom exponent and bimodal aerosol size distributions. J. Geophys. Res., 2006, 111. http://dx.doi.org/10.1029/2005JD006328.

[20] Marey, H.S., Gille, J.C., El-Askary, H.M., Shalaby, E.A., El-Raey, M.E. Aerosol climatology over Nile Delta based on MODIS, MISR and OMI satellite data. Atmos. Chem. Phys., 2011, 11, 10637–10648.

[21] Marey, H.S., Gille, J.C., El-Askary, H.M., Shalaby, E.A., El-Raey, M.E., Study of the formation of the "black cloud" and its dynamics over Cairo, Egypt, using MODIS and MISR sensors. J. Geophys. Res. 2010, 115, D21.

[22] El-Askary, H., Air pollution impact on aerosol variability over mega cities using remote sensing technology: Case study, Cairo, Egypt. Egypt. J. Remote Sens. Space Sci., 2006, 9, 31–40.

[23] El-Askary, H., Kafatos, M., Dust storm and black cloud influence on aerosol optical properties over Cairo and the Greater Delta region, Egypt. Int. J. Remote Sens. 2008, 29, 7199–7211.

[24] Prasad, A.K., El-Askary, H., Kafatos, M., Implications of high altitude desert dust transport from Western Sahara to Nile Delta during biomass burning season, Environ. Pollut. 2010, 158, 3385–3391.

[25] El-Askary, H., Farouk, R., Ichoku, C., Kafatos, M., Transport of dust and anthropogenic aerosols across Alexandria, Egypt, Ann. Geophys. 2009, 27, 2869–2879.

[26] El-Metwally, M., Alfaro, S.C., Abdel Wahab, M., Chatenet, B., Aerosol characteristics over urban Cairo: Seasonal variations as retrieved from Sun photometer measurements, J. Geophys. Res. 2008, 113, D14.

[27] El-Metwally M., S.C. Alfaro, M.M. Abdel Wahab, O. Favez, Z. Mohamed, B. Chatenet, Aerosol properties and associated radiative effects over Cairo (Egypt), Atmospheric Research February 2011, 99(2): 263-276.

[28] Islam Abou El-Magd, Naglaa Zanaty, Elham M. Ali, Hitoshi Irie, and Ahmed I. Abdelkader, Investigation of Aerosol Climatology, Optical Characteristics and Variability over Egypt Based on Satellite Observations and In-Situ Measurements. Atmosphere, 2020, 11, 714; doi:10.3390/atmos11070714.

[29] Wenzhao Li, Elham Ali, Islam Abou El-Magd, Moustafa Mohamed Mourad and Hesham El-Askary, Studying the Impact on Urban Health over the Greater Delta Region in Egypt Due to Aerosol Variability Using OpticalCharacteristi cs from Satellite Observations and Ground-Based AERONET Measurements, Remote Sens., 2019, 11, 1998; doi:10.3390/rs11171998.

[30] Rabie M. M., Kh. O. Kassem, A. A. Hassan, B. Nobi, Study of the suspended particulate matter concentrations in the atmosphere of Qena, Upper Egypt. Master Thesis, Faculty of science, SVU.

[31] Kassem Kh. O., A. A. Hassan, B. Nobi, Rabie M M, Morphological and Chemical Composition of Total Particulate Matter in Region of Qena/ Egypt, IOSR Journal of Environmental Science, Toxicology and Food Technology (IOSR-JESTFT), 2018, Volume 12, Issue 8 Ver. I (August. 2018), PP 29-36.

[32] Kassem Kh. O., Long Range Transport Contribution to PM10 Concentrations in a Subtropical City (Qena/Egypt), World Environment, 2014, 4(1): 1-13.

[33] Zakey, A.S., Abdel-Wahab, M.M., Pettersson, J.B.C., Gatari, M.J., Hallquist, M., Seasonal and spatial variation of atmospheric particulate matter in a developing megacity, the Greater Cairo, Egypt, Atmósfera, 2008, 21, 171189.

[34] Kassem, Kh. O., Abdel-Azeam M. A., Sayed M. E., Masaaki T., Mahmoud E.A., Variability of surface ozone in some regions in Egypt. Ph.D. PHYSICS, 2009, the faculty of science, Qena, south valley university.

[35] Soni, K., Singh, S., Bano, T., Tanwar, R.S., Nath, S., Wavelength Dependence of the Aerosol Angstrom Exponent and Its Implications Over Delhi, India., Aerosol Sci. Tech. 2011, 45, 1488–1498.

[36] Kolhe, A.R., Pawar, G.V., Varpe, S.R., Kumar, P.P., Devara, P.C.S., Aher, G.R., Multi-Year Analysis of Aerosol Properties Retrieved from the Å ngström Parameters for Different Spectral Ranges over Pune., Aerosol. Air Qual. Res. 2017, 16, 3266–3280.

[37] Kaskaoutis D. G., H. D. Kambezidis, N. Hatzianastassiou, P. G. Kosmopoulos, and K. V. S. Badarinath, Aerosol climatology: dependence of the Angstrom exponent on wavelength over four AERONET sites. Atmos. Chem. Phys. Discuss., 2007, 7, 7347–7397, www.atmos-chem-phys-discuss.net/7/7347/2007/.

[38] Reid, J. S., T. F. Eck, S. A. Christopher, P. V. Hobbs, and B. N. Holben, Use of the Angstrom exponent to estimate the variability of optical and physical properties of aging smoke particles in Brazil, J. Geophys. Res., 1999, 104, 27,473 – 27,489.

[39] Eck, T. F., B. N. Holben, D. E. Ward, O. Dubovik, J. S. Reid, A. Smirnov, M. M. Mukelabai, N. C. Hsu, N. T. O'Neill, and I. Slutsker, Characterization of the optical properties of biomass burning aerosols in Zambia during the 1997 ZIBBEE Field Campaign, J. Geophys. Res., 2001, 106, 3425 – 3448.

[40] Eck,T. F., B. N. Holben, O. Dubovik, A. Smirnov, P. Goloub, H. B. Chen, B. Chatenet, L. Gomes, X.-Y. Zhang, S.-C. Tsay, Q. Ji, D. Giles, and I. Slutsker, Columnar aerosol optical properties at AERONET sites in central eastern Asia and aerosol transport to the tropical mid-Pacific, JOURNAL OF GEOPHYSICAL RESEARCH, 2005, VOL. 110, D06202, doi:10.1029/2004JD005274.